QUARTERLY JOURNAL OF THE ROYAL METEOROLOGICAL SOCIETY

Q. J. R. Meteorol. Soc. **00**: 1–18 (2008)

Published online in Wiley InterScience

(www.interscience.wiley.com) DOI: 10.1002/qj.000

Modulation of tropical convection by breaking Rossby waves

G. Allen[a]*G. Vaughan[a], D. Brunner[b], P. T. May[c], W. Heyes[a], P. Minnis[d], J. K. Ayers[d]

¡[a]*Centre for Atmospheric Science, University of Manchester, Oxford Rd, Manchester, M13 9PL, UK*

[b]*EMPA, Swiss Federal Institute for Materials Testing and Research, Dubendorf, Switzerland*

[c]*Centre for Australian weather and climate research, Melbourne, Australia*

[d]*NASA Langley Research Center Science Directorate, Hampton, VA, USA*

Abstract: This work discusses observations of both the convective-inhibiting and convective-promoting abilities of breaking Rossby waves in the tropics. Two tropical drought periods - times of reduced tropical cloudiness and rainfall - were observed during mid-to-late November 2005 over a wide area of North-West Australia, with the eruption of a nearby synoptic tropical cloud plume observed in between times. Both convective inhibition and promotion appear to be linked to the descent of dry upper tropospheric air within a series of tropopause folds; with convective inhibition observed within the dry pool itself, and promotion observed on the high moisture gradient at the leading edge of an advancing dry slot. A range of satellite imagery, surface rain gauges, radiosonde and ozonesonde data are used in conjunction with back trajectories and ECMWF analysis fields to investigate the origins and dynamics associated with these convective events, showing each to be ultimately linked to breaking Rossby wave activity on the Southern Subtropical Jet. Together, these observations support a growing number of studies linking midlatitude tropopause-level dynamics with the modulation of tropical deep convection, an influence that is poorly characterized when considering the climatology of tropical cloudiness and rainfall. Copyright © 2008 Royal Meteorological Society

KEY WORDS Convection; Tropopause Fold; Rossby Wave; Stratosphere to Troposphere Exchange

Received 5 May 2008; Revised ; Accepted

1 Introduction

Deep convection in the tropics is one of the main engines of the general circulation, and is one of the most difficult processes to represent correctly in general circulation models. A thorough understanding of the large-scale influences on tropical convection is therefore a prerequisite for successful modelling of the atmosphere. In this paper we examine the role of breaking Rossby waves generated along the Subtropical Jet-stream (STJ), but in their final form extending well into the tropics, on the distribution of deep convection over North West Australia. These waves generate characteristically filamentary structures in the horizontal, taking the form of tropopause folds in the vertical dimension. Folds can extend well down into the troposphere, setting up deep dry layers of enhanced static stability, which act as lids on any upwelling convection. Conversely, if such dry layers over-run layers of moist boundary layer air, convection may result if sufficient forcing is available to release the potential instability generated by the layers (see Section 4.2).

*Correspondence to: Centre for Atmospheric Science, University of Manchester, Oxford Rd, Manchester, M13 9PL, UK

The notion of a "tropical drought" was introduced by Mapes and Zuidema (1996). Here we examine two tropical drought events, separated by a period of enhanced convective activity, which occurred over North West Australia in November 2005 (during the wet season) and relate them to the passage of breaking Rossby waves.

Breaking Rossby waves and associated tropopause folds are ubiquitous features of upper tropospheric meteorology, and are reasonably well understood theoretically (e.g. Hoskins and Ambrizzi (1993)). Less well understood is their influence on lower level dynamics; specifically their ability to modulate convection. Previous case studies of convective modulation by upper level PV anomalies have reported that both convective destabilization and convective inhibition can be induced under different circumstances. For example, developing convection may be effectively halted (by droplet evaporation) if sufficiently dry surrounding air is entrained into developing cloud, as suggested by Mapes and Zuidema (1996). However, if a dry layer is present at the top of the boundary layer, over a sufficiently moist layer, the resulting potential instability may instead promote convection if sufficient boundary layer forcing (convergence) is present (e.g. Browning and Roberts (1994; 1995)).

The radiative-dynamic implications of dry layers (or tongues) in the tropical maritime troposphere was discussed by Mapes and Zuidema (1996), and Parsons (2000), using measurements made during the TOGA COARE field campaign centred on the Solomon Islands. Although not attributed directly to tropopause folding, they showed that commonly observed dry layers over the Tropical Western Pacific (TWP), advected from the subtropical upper troposphere, were correlated with periods of reduced precipitation and reduced occurrence of deep convection. The entrainment of dry air in the free troposphere was cited as a likely cause of convective suppression, coupled with strong radiatively-induced thermal inversions as a result of the high gradient in water vapour concentration at the bottom of such dry layers. Further analysis of the origins of dry layers over the TWP by Yoneyama and Parsons (1999) showed that dry air advected to the TWP was transported in baroclinic waves of NH sub-tropical origin and in one case by a breaking Rossby wave on the SH Subtropical Jet (STJ). A later, more detailed case study of a dry-tongue event during TOGA COARE by Parsons *et al.* (2000), albeit limited to the maritime troposphere, again showed a marked and correlated reduction in rainfall and convective activity, and reported that radiatively-induced convective inhibition (CIN) alone may (unusually) be enough to suppress convection in the TWP. However, they highlighted the need for further studies of this type to confirm such findings and noted the need for a correction to their radiosonde dataset, not available at that time.

The ability of tropopause folds to promote deep convection through potential instability was recognised as far back as Danielsen (1968), and there have been a number of studies in the literature of this phenomenon (e.g. Browning and Roberts (1994; 1995)]; Morcrette *et al.* (2007)). Indeed, the paradigm introduced by Hoskins *et al.* (1985), that upper-level PV anomalies destabilise the atmosphere beneath them would suggest that tropopause folds always induce convection. By this mechanism, a tropopause fold generates regions of potential instability when dry layers inherent to folds overlay layers of moist air at lower levels, thus leading to a decreasing wet-bulb potential temperature profile with height. The release of such potential instability (through convection) requires sufficient forced

DOI: 10.1002/qj

ascent of the lower layer; for example by topographic forcing or sea-breeze convergence. However, such forcing is not always present and therefore the potential instability generated by tropopause folds may not always be realised. Several other studies have linked Rossby wave propagation into the tropics with the promotion of deep convection (e.g. Slingo (1998); Kiladis (1998); Yoneyama and Parsons (1999); Knippertz (2005)). So-called Tropical Plumes (TPs), or SW-NE-orientated (in the NH) synoptic-scale cloud bands stretching from the tropics to the subtropics (or even the midlatitudes), have been found to coincide with mobile upper-level troughs (e.g. Knippertz and Martin (2006)); such troughs take the form of elongated stratospheric PV streamers or cut-offs linked to the crests of breaking Rossby waves. However, as noted by Knippertz (2007), there is some question in the literature regarding the physical processes involved in the relationship between TPs and upper-level troughs at low latitude - the key question being whether observed lifting is a result of dynamical forcing, convective heating or some interaction of the two.

A ubiquitous feature of a TP is a very dry (dark) tongue in water vapour (WV) satellite imagery to the northwest (southwest in the SH) of the TP (e.g. Blackwell (2000); Knippertz (2005)). The gradient in mid-to-upper-level moisture between these dry and moist zones has been found to be very high in composites of TPs over the NH Pacific by McGuirk and Ulsh (1990). Consistent with the observation of such dry tongues, McGuirk *et al.* (1988) and Blackwell (2000) found subsidence at mid-levels in such areas. Dry air from the subsidence region of a low-latitude trough and TP has previously been observed to intrude deep into the Tropics and influence conditions for convection over the western Pacific as shown by the case study of Yoneyama and Parsons (1999).

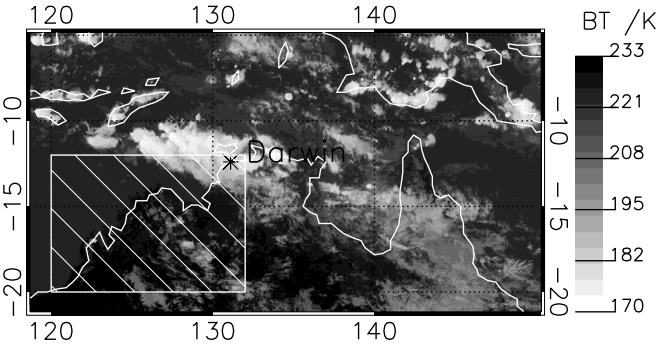

Figure 1. Grey-scale image of MTSAT-1R water vapour channel brightness temperatures (BT) over Northern Australia at 05:30 UTC on 20 November 2005, showing a cloud-plume over Darwin. The cross-hatched area defines the ROI. Dark areas indicate dry air at mid-levels.

In this work, we will discuss several dry tongues in the troposphere associated with a series of tropopause folds, and discuss the various observed effects on convective activity over North West Australia through the synergistic use of ozone and radiosondes and surface rain gauges, compared with satellite-derived cloud information and imagery and ECMWF reanalysis data.

2 Data and methodology

For the purposes of this case study, we confine our analysis to the one month period between 10 November and 10 December 2005, to make full use of the intensive observation period of the ACTIVE aircraft campaign (see following section), conducted from Darwin, Australia (12.46 °S, 130.93 °E). Furthermore, a region of interest (herein referred to as the ROI) over tropical NW Australia is defined between 120 °E to 133 °E and 12 °S to 20 °S, based on MTSAT-1R satellite observations of a prevalent dry slot during the drought period. The ROI is indicated by the diagonally-hatched area in Figure 1 - the dry tongue over the ROI seen as a dark area in the water vapour field.

2.1 The ACTIVE campaign

Ozonesonde and meteorological data discussed here were recorded as part of the UK Aerosol and Chemical

DOI: 10.1002/qj

Transport in tropical conVEction (ACTIVE) campaign, described further by Vaughan *et al.* (2008). This campaign was conducted during the 2005/2006 wet season (November - February) from Darwin, Australia, as part of an extensive field campaign to study tropical convection and its effect on the Tropical Tropopause Layer (TTL), in tandem with the Stratospheric-Climate Links with Emphasis on the Upper Troposphere and Lower Stratosphere (SCOUT-O3) campaign (also described by Vaughan *et al.* (2008)).

2.2 Vertical soundings from Darwin

During November 2005, Vaisala RS80 radiosondes were launched twice daily at 1100 UTC (2030 local) and 2300 UTC (0830 local) from Darwin Airport by the Australian Bureau of Meteorology (BoM). Pressure, humidity, wind and temperature data were recorded every 10 seconds during ascent, giving a vertical resolution of roughly $20\ m$ on average in the troposphere. On days of scientific interest to ACTIVE or SCOUT-O3, electrochemical concentration cell (ECC) ozonesondes were added to the radiosonde payload and a Vaisala RS92-KE sonde was used instead of the RS80. Following Reid *et al.* (1996), we applied a constant background current correction to the ozonesonde measurements in the troposphere, rather than the standard pressure-varying correction. Measured ozonesonde profiles were consistent ($\pm$ 5 ppbv) with ozone profiles recorded by the SCOUT-O3 Geophysica aircraft. A total of 29 such ozonesondes were launched from Darwin airport during the ACTIVE campaign, with 5 available during the drought period of interest to this study.

2.3 ECMWF Analyses

Wind, pressure, temperature, specific humidity and vertical motion fields used here were taken from data hosted by the British Atmospheric Data Centre (BADC) and produced by the European Centre for Medium Range Weather Forecasting (ECMWF) operational analysis Integrated Forecasting System (IFS Cycle 29r2). The above fields were provided on a $1.125\,^\circ \times 1.125\,^\circ$ grid on 60 hybrid model levels. Isentropic fields of these variables were constructed by interpolation between model levels. Isentropic potential vorticity (PV) fields were calculated by linearly interpolating winds and static stability onto isentropic surfaces, then calculating PV from these fields.

2.4 Satellite data

The Japanese Meteorological Agency Multi-functional Transport Satellite (MTSAT-1R), launched on 26 February 2005, is a geostationary satellite providing coverage for the hemisphere centred on $140\,^\circ$E. It provides imagery in five wavelength bands: one visible ($0.55 - 0.80\ \mu m$), two infrared ($10.3 - 11.3\ \mu m$; $11.5 - 12.5\ \mu m$), one near infrared ($3.5 - 4.0\ \mu m$) and a further infrared channel sensitive to water vapour ($6.5 - 7.0\ \mu m$). The visible and infrared cameras have spatial resolutions of $1\ km$ and $4\ km$ at the nadir point respectively (resolution is lower away from the equator and at $140\,^\circ$E). A portion of an MTSAT-1R water vapour channel image is shown in Figure 1. Cloud data products used in this study were retrieved from MTSAT-1R imagery (Minnis *et al.* (2006)), using the Visible Infrared Solar-Infrared Split Window Technique (VISST) and the Solar-Infrared Infrared Split Window Technique (SIST) method of Minnis *et al.* (1995). This method uses MTSAT-1R brightness temperatures in all channels during daytime (VISST) and night-time (SIST) in conjunction with other available satellite and meteorological observations to derive information on cloud top height, cloud phase, cloud thickness and other parameters.

DOI: 10.1002/qj

2.5 Surface Rain-gauges

This tropical location also benefits from the presence of a comprehensive rain gauge network operated by the Australian Bureau of Meteorology (BoM) across Australia's Northern Territory. The region of interest discussed in this work contains a total of 643 203 mm capacity rain gauges read daily at 0900 local time. This study uses a $0.5^\circ \times 0.5^\circ$ gridded rainfall product derived from all available rain gauges, provided by the BoM.

3 Meteorological Context

A comprehensive description of the meteorology affecting the Darwin area during the ACTIVE/SCOUT-O3 campaign between early November and late December 2005 is given by Brunner *et al.* (2008)). In summary, the wet season in northern Australia typically starts in October with the pre-monsoon "build-up" period characterized by weak easterly trades at low levels and a strong diurnal evolution of isolated storms and mesoscale systems typical of continental tropical convection. Throughout early -to mid-November 2005, typical pre-monsoon conditions were observed over the ROI, with local sea-breeze circulations generating a range of convective storms; from isolated thunderstorms to squall line complexes $100\ km$ in scale. Such deep convective storm systems regularly achieved cloud top heights in excess of $18\ km$ (Vaughan *et al.* (2008)). A low-level trough moved east over the Northern Territory between 19 and 23 November in an exception to the general pattern, causing a reversal in the convective steering level wind direction from prevailing easterlies to a deep westerly flow from 700 hPa to 200 hPa. This feature was local in scale and occurred well away from the ITCZ.

4 Observations and results

Here, we will discuss the broad convective character of two drought periods over the ROI during November 2005, focussing on the latter of the two drought periods in the context of a case study, before discussing observations of a tropical plume to the north of the ROI, which occurred between these two dry periods.

4.1 A tropical drought over Northern Australia

4.1.1 Convective characteristics over the ROI

During two periods between 16 to 19 November and 23 to 27 November 2005, much reduced cloud cover and precipitation was observed over the ROI. A time sequence of satellite-observed fractional cloud cover over the ROI, together with area-averaged ECMWF-derived PV and vertical motion evaluated at 325 K potential temperature (mid-troposphere) is plotted in Figure 2a. A corresponding time-series of daily-accumulated surface rain gauge data averaged over the ROI, together with ECMWF forecast rainfall and ECMWF Relative Humidity (RH) evaluated at 325 K is plotted in Figure 2b. Together, Figures 2a and 2b show a marked reduction in measured rainfall over the area during these two periods, herein referred to as Drought Periods 1 and 2, or DP1 and DP2, respectively. Both drought periods coincided with peaks in PV and positive vertical motion (in pressure coordinates) indicating large-scale down-welling. Note that the modulus of PV is used herein, but that PV is negative by convention in the SH. As might be expected, reductions in RH coincide with the periods of descent. During DP2, cloud cover is also seen to be much reduced ($< 2\%$ over the ROI). Conversely, cloud cover appeared to remain fairly constant during DP1, although in general such cloud appears to be non-precipitating based on rain gauge data. On closer

DOI: 10.1002/qj

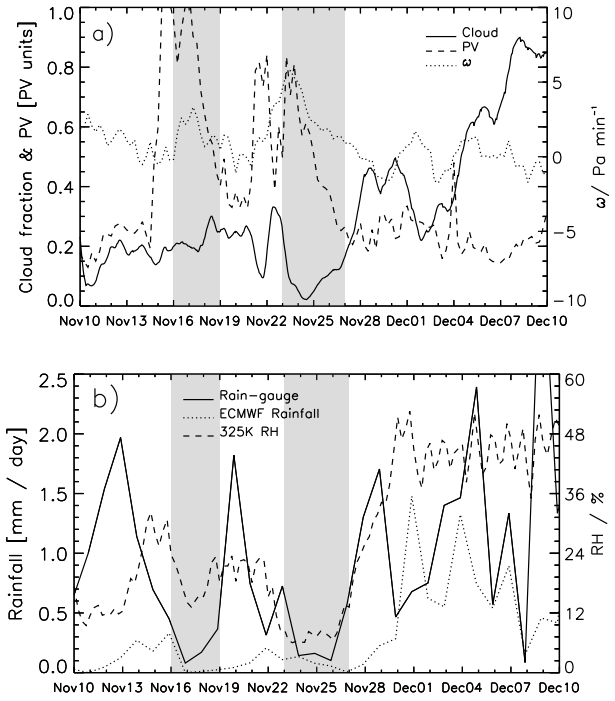

Figure 2. Time series of: a) Fractional area of the ROI covered by cloud inferred from MTSAT-1R imagery, with area-averages of ECMWF-derived potential vorticity (absolute value, in PV units) and vertical motion (ω) on the 325 K isentrope; and b) Accumulated daily rainfall measured by surface rain gauges with area-averaged ECMWF surface rainfall and Relative Humidity (RH) on the 325 K isentrope. Shaded areas show two drought periods (see text for details)

inspection of MTSAT-1R Channel 1 brightness temperatures, we note that much of the cloud observed during DP1 was found at high levels (low brightness temperature) and advected from deep convective systems upstream of the ROI.

It is interesting to note that in each of the two dry periods, rainfall remained low even after the area-averaged PV signature returned to baseline values.

A sequence of cloud-top-height (CTH) maps derived from MTSAT-1R brightness temperatures over the ROI is shown in Figure 3 illustrating the vigour of convective activity in the area before, during and after DP2. In each case, CTH observations are shown at 3 pm local time (0530 UTC), the approximate time of peak convective activity. Before DP1, in the typical case of 14 November (Fig 3(a)), there is widespread convection along the coast and inland, with CTH reaching in excess of 16 km. However, during DP2 (Figures 3(b), 3(c), 3(d)), we see greatly reduced convective activity over the area, with remaining convection confined to coastal regions, where strong sea-breeze convergence is found, with slightly lower cloud heights of 14 km at maximum. A return to typical wet season convection occurs on 28 November (Fig 3(e)) with widespread land and coastal cells. This picture of reduced cloudiness and rainfall during periods of large-scale descent and low mid-level humidity is not surprising. However, the high PV associated with the descending airmass seen here indicates a tropopause-level origin (as we shall discuss in the following section) and hence isentropic transport from higher latitudes.

4.1.2 *Upper level dynamics affecting the ROI during DP2*

Potential vorticity and wind vector maps derived from ECMWF analyses are plotted in Figure 4 for the 335 K isentrope (approximately 360 hPa over Darwin) showing a time-evolution of these fields in the upper troposphere over the Indian Ocean and Australia during DP2. On 20 November, a breaking Rossby wave on the Subtropical Jet (STJ), defined by the region with the highest PV gradient (blue in Fig 4(a)), developed over South West Australia. By 22 November, the wave had moved eastward, with evidence of a double-breaking event on the STJ, seen as two closely-spaced wave peaks in Figure 4(b). A streamer of high PV extended westward over the ROI from the first wave peak. By 23 November the second of the two breaking waves extended toward the equator with a near north-south orientation (Figure 4(c)) and moved eastward across the ROI. The greater penetration of this wave to lower latitudes appears to have been assisted by the westerly momentum imparted at lower latitudes by the preceding breaking event, consistent with the findings of Davidson

DOI: 10.1002/qj

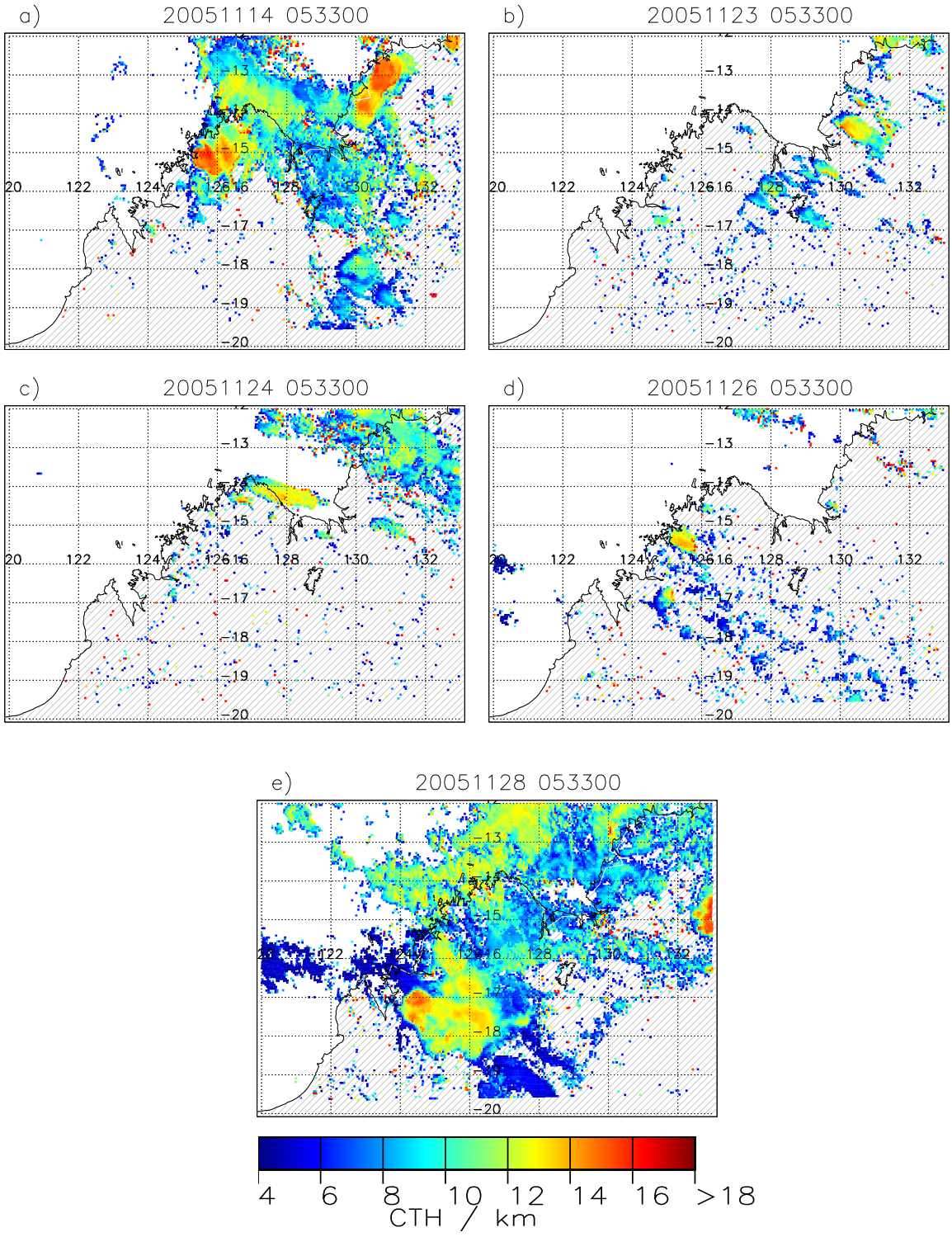

Figure 3. Cloud top heights (km) derived from MTSAT-1R infrared brightness temperatures within the region of interest for the dates specified in each panel at 0533 UTC (1433 local time)

et al. (2007) and earlier studies, which show that wave propagation is favourable in an embedded westerly flow. Furthermore, an upper level anti-cyclone formed in the lee of the wave to the west (see Figure 4(c)), which acted to stretch a streamer of high PV over the ROI extending from the breaking wave. By 25 November, this upper level anti-cyclone (upper level ridge) had moved over the ROI marking an area of large-scale downward motion, while the STJ had retreated southward (Figure 4(d)), leaving residual PV ($\sim -0.7\ PVU$) over much of the ROI. A quiescent STJ

Prepared using qjrms3.cls
DOI: 10.1002/qj

was re-established to the South on 27 November (Figure 4(e)). Vertical cross-sections of PV, RH and potential temperature isentropes through the 125 °E meridian (centre of the ROI) are plotted in Figure 5 and reveal the vertical structure of the tropopause fold associated with the double breaking event as it passed over the ROI during DP2. The 335 K isentrope can be used to relate fields plotted in Figure 5 with those plotted in Figure 4. Before the Rossby wave crossed this meridian on 20 November (Fig 5(a)), the STJ lay south of the ROI. On 22 November (Fig 5(b)) the elongated PV streamer associated with the first wave of the double-breaking event noted earlier and seen in Figure 4(b) is observed at 15 °S, with the spatially separated fold of the second breaking event seen at 18 °S. On 23 November a finger of high PV (~ 1 PVU), low relative humidity air ($< 10\%$) descended from upper levels beneath the northernmost jet (Figure 5(c)). This finger is a tropopause fold, which gradually diminished in prominence over the next two days, before a quiescent jet-stream was seen to the south on 27 November (Figure 5(e)). The dry air transported from the upper troposphere within the fold continued to be evident over the ROI well after its PV signature had been lost. A pool of very dry (less than 10% RH) air resided over the ROI for the period 23 to 27 November, correlated with the period of reduced cloud cover and precipitation shown in Figure 2.

It is important to discuss here the convention in defining tropopause folds. In many of the midlatitude studies discussed earlier, a tropopause fold is defined by the position of the 2 PVU surface, since this is a useful definition of the dynamical tropopause in the extra-tropics. However, when considering the spatial extent of stratospherically-influenced airmasses in this study (see Figure 4), we see that anomalous PV and associated dry air extends well beyond the 2 PVU surface. In the following section, we will show that air sampled within layers displaying PV as low as 0.5 PVU in ECMWF analyses retains significant stratospheric chemical characteristics.

4.1.3 *Vertical soundings and back trajectories*

Ozonesondes launched from Darwin Airport during the passage of the fold (see Figure 6) showed very dry layers with enhanced ozone concentration in the mid-troposphere. Such high ozone concentrations and anti-correlated water vapour are characteristic of tropopause folds. At 0500 UTC (1430 local) on 22 November at Darwin (Figure 6(a)), a layer of enhanced ozone (up to 130 ppbv) and reduced RH ($< 10\%$), was observed between 390 hPa and 530 hPa; or 336 K and 322 K potential temperature, respectively. Comparing this with Figure 4(b) and 5(b), we see that this layer is associated with the first of the breaking waves on a day when rainfall and cloud cover were reduced over the ROI (recall Figure 2). On 23 November (Figure 6(b)), there were thin layers of enhanced water vapour and reduced ozone in the mid-levels, characteristic of convective uplift and outflow, with another thin layer of ozone-rich dry air at 350 mb (338 K) which also had high static stability (not shown). On 24 November (Figure 6(c)), the convective signature was absent but a pronounced very dry layer ($< 10\%$ between 430 mb [262 K] and 520 mb [325 K]) was observed, coincident with increases in ozone up to 100 ppbv. This dry layer deepened and thickened by the 27th (Figure 6(d)), before a return to a more climatological humidity and ozone profile on 30 November (Figure 6(e)), with convective detrainment layers once more evident in the measured profile. Figure 7 shows four-day, 3-D back trajectories ending at 500 mb in a cluster around 12.4 °S, 130.9 °E (Darwin) at times corresponding to the ozonesonde profiles in Figure 6. The three profiles with enhanced ozone layers (22, 24 and 27 November) show

DOI: 10.1002/qj

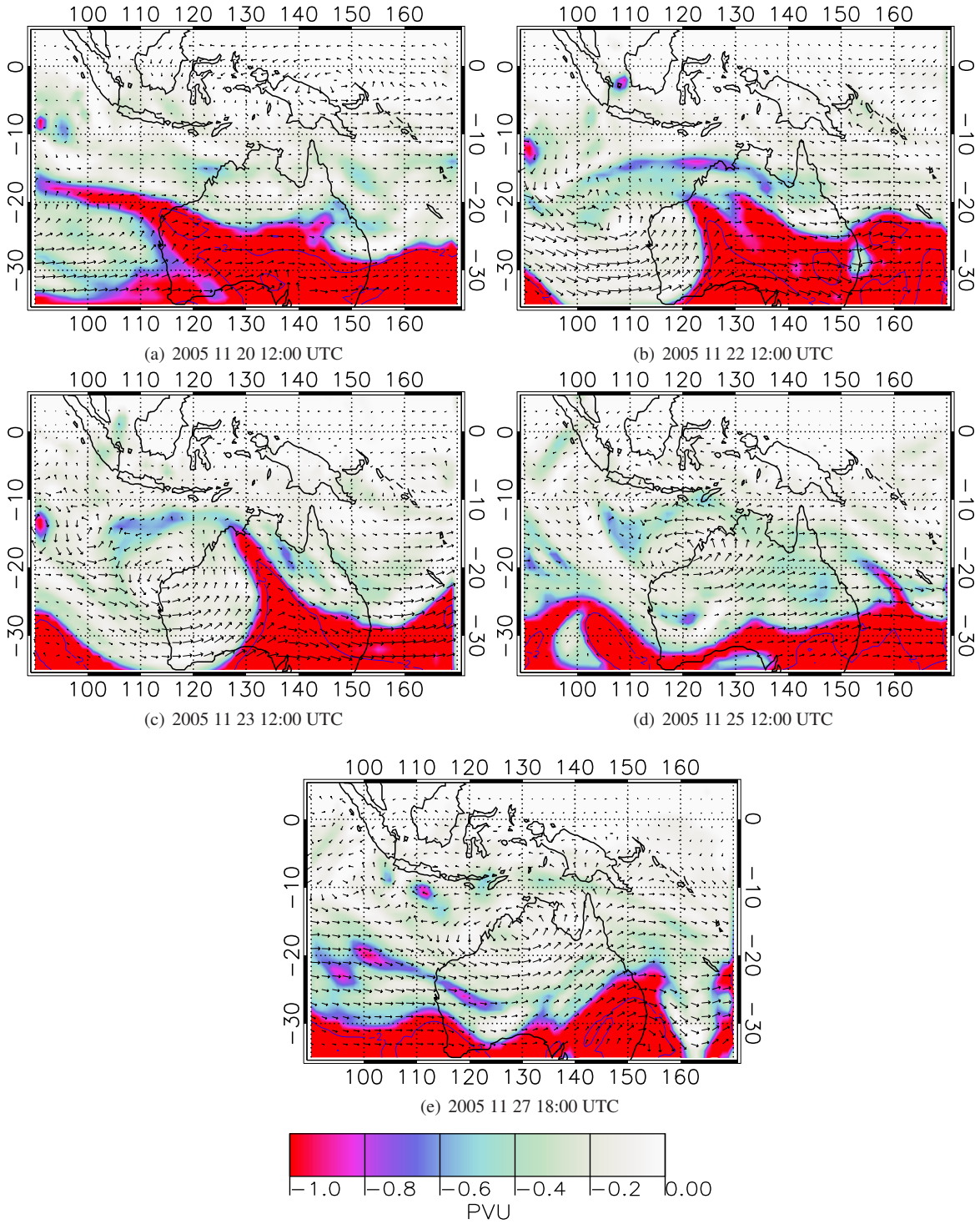

Figure 4. Isentropic (335 K) potential vorticity (colour contours) and wind fields (arrows) derived from ECMWF analyses over the Australian synoptic area for the times indicated in each panel. The solid blue contour indicates the -2 PVU surface.

little dispersion within the trajectory clusters, allowing an estimate of air parcel origin. On 22 November, when the highest ozone concentration during this period was measured (130 ppbv), four of the five trajectories originated from the PV filament extending westward from the breaking Rossby wave. On 27 November the cluster originated from the tip of the PV streamer wrapping anticlockwise around the upper level anticyclone west of Australia, while on 24 November the cluster originated from the tropospheric side of the jet stream around 30 °S,

Prepared using qjrms3.cls
DOI: 10.1002/qj

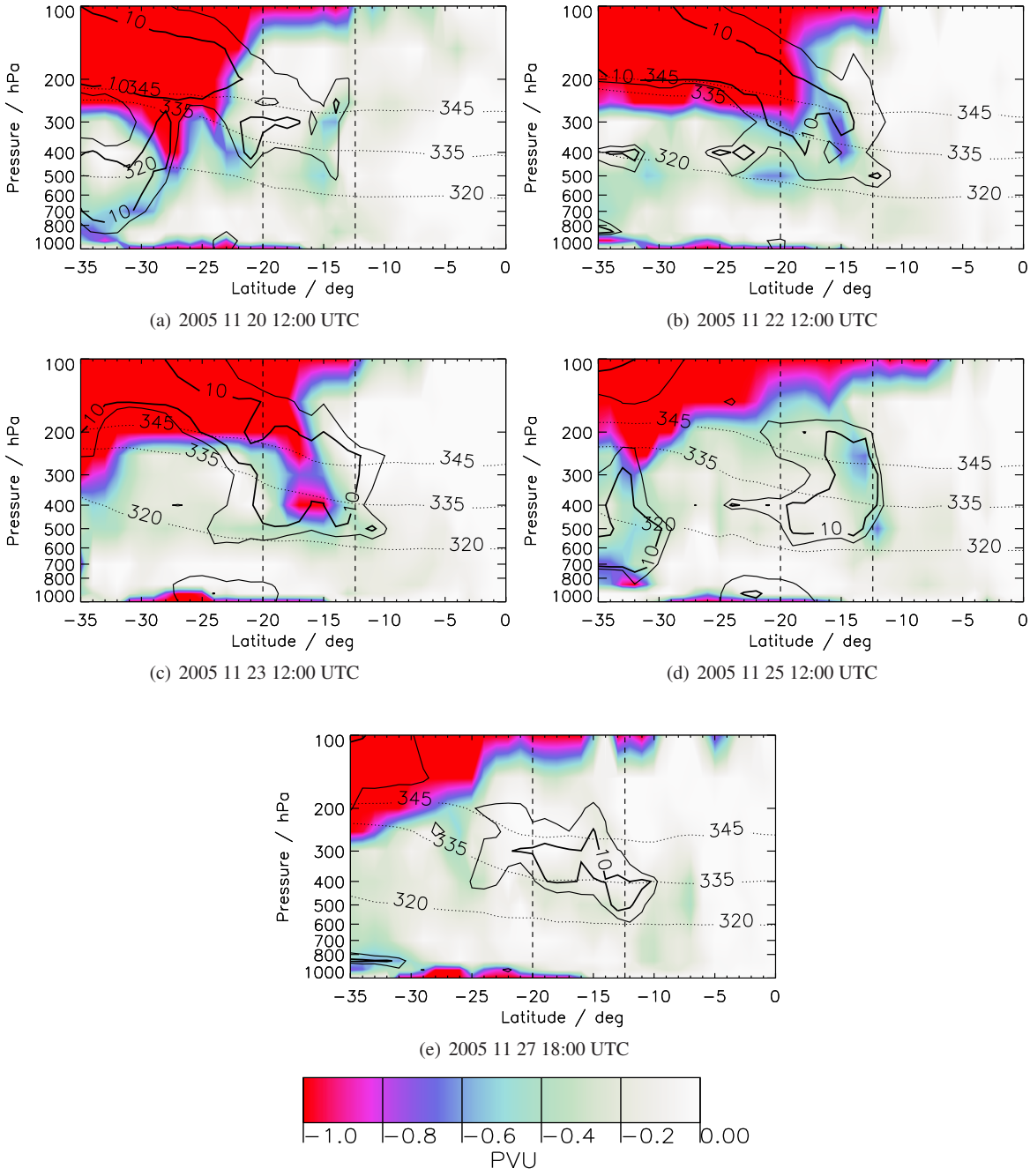

(a) 2005 11 20 12:00 UTC

(b) 2005 11 22 12:00 UTC

(c) 2005 11 23 12:00 UTC

(d) 2005 11 25 12:00 UTC

(e) 2005 11 27 18:00 UTC

Figure 5. Vertical-latitudinal cross-sections through the 125 °E meridian of: PV (colour contours), the 10% and 20% RH area (solid black contours) and potential temperature surfaces at 320, 335 and 345 K (dotted contours) for the dates specified in each panel. Dashed vertical lines indicate the latitudinal bounds of the ROI.

100 °E. On 23 November, the cluster diverges - two trajectories originate from the stratosphere and the other three remain in the troposphere ahead of the breaking Rossby wave. Divergence of the cluster means the air parcel origin cannot be inferred for this day. Finally, on 30 November when the profile is again free of ozone-rich dry layers, the cluster remains in the troposphere with no connection to a PV filament. This analysis is consistent with a stratospheric origin for the layers on 22 and 27 November, and a tropospheric origin on 30 November. For the 24 November the cluster originated equatorward of the STJ in a region of PV in the range -0.4 to -0.7 PVU. This range is similar to that at the trajectory end-points

DOI: 10.1002/qj

on 22 and 27 November, confirming the point made above that air with a clear chemical signature corresponded to absolute PV values much less than 2 PVU. One reason for this is the inability of the ECMWF analysis to represent thin layers - on 22 and 23 November the ozone-rich dry layers coincided with high static stability. However, on 24 and 27 November static stability was not enhanced, suggesting a genuine loss of potential vorticity consistent with the conclusion of Bithell *et al.* (2000) that layers of stratospheric air entrained into the troposphere retain their chemical signature far longer than their enhanced PV (or static stability).

4.2 Observations of a Tropical Plume

In the period between DP1 and DP2 (20-22 November), an eruption of convective activity occurred to the north of the ROI, predominantly over the Arafura Sea to the west of Darwin. A time sequence of the first of these convective events is plotted in Figure 8, which shows false-colour water vapour channel images recorded by MTSAT-1R. Convection was initiated at 2200 UTC on 19 November (0730 local time on 20 November) on the western coast of Australia at 129.5 °E, 15.6 °S (marked with a cross on Figure 8(a)), seen as isolated bright white points. These initially isolated convective cells were observed within an eastward advancing dry slot (seen as the brown/dark area in Figure 8(a)). The fact that this convection occurred only shortly after local sunrise, and on the coast, suggests that it was not forced by solar heating of the continental boundary layer and rather represents a dynamically-forced release of potential instability.

Figures 8(b) to 8(h), recorded at one-hourly intervals, show the rapid development of a line of deep convection spreading to the north and west from the initial point on the coast, near the boundary between the moist and dry airmasses. Over a period of 6 hours, this convective line developed to span 6 degrees of longitude across tropical latitudes, resembling the pattern of a synoptic scale tropical plume (herein referred to as a TP) as described earlier in Section 1. The rapid development of this line over such a large distance rules out self-propagation (by gust-front forcing for example) - the required phase speed would be of the order $40\ ms^{-1}$ and therefore too fast for such processes. Furthermore, Figures 8(f) and 8(g) show isolated development of convective cells to the north-east of the main plume along the moist/dry boundary, which later became part of the plume (Figure 8(h)). These isolated cells further suggest that the convective line was not dynamically linked to the initial convection, but does demonstrate a causal link associated with the dry/moist airmass boundary. This link is now investigated further.

4.2.1 Thermodynamics of the plume

Figure 9 shows Convective Available Potential Energy (CAPE) and Convective Inhibition Energy (CIN), derived here for surface air from ECMWF thermodynamic profiles on 60 model levels at 00 UTC (0930 local time) on 20 November 2005, corresponding to the satellite image in Figure 8(c). We see, from Figure 9(a), that there is a region of high CAPE to the north and east of the convective line observed in Figure 8 and a region of very low CAPE to the south and west. The region of low CAPE over the ocean to the west of the plume is coincident with a region of high CIN (up to $400\ Jkg^{-1}$), coinciding with the eastward advancing dry slot seen in the satellite images of Figure 8. Hence, we see that the observed convective plume was initiated within a region of high convective inhibition ($\sim 200\ Jkg^{-1}$), but significant CAPE ($\sim\ 2000\ Jkg^{-1}$) on the leading edge of the advancing dry slot. It is also noteworthy that CIN was very low ($< 50\ Jkg^{-1}$) and CAPE very high over the northern tip of Australia at this time, but deep convection was not initiated there, suggesting

DOI: 10.1002/qj

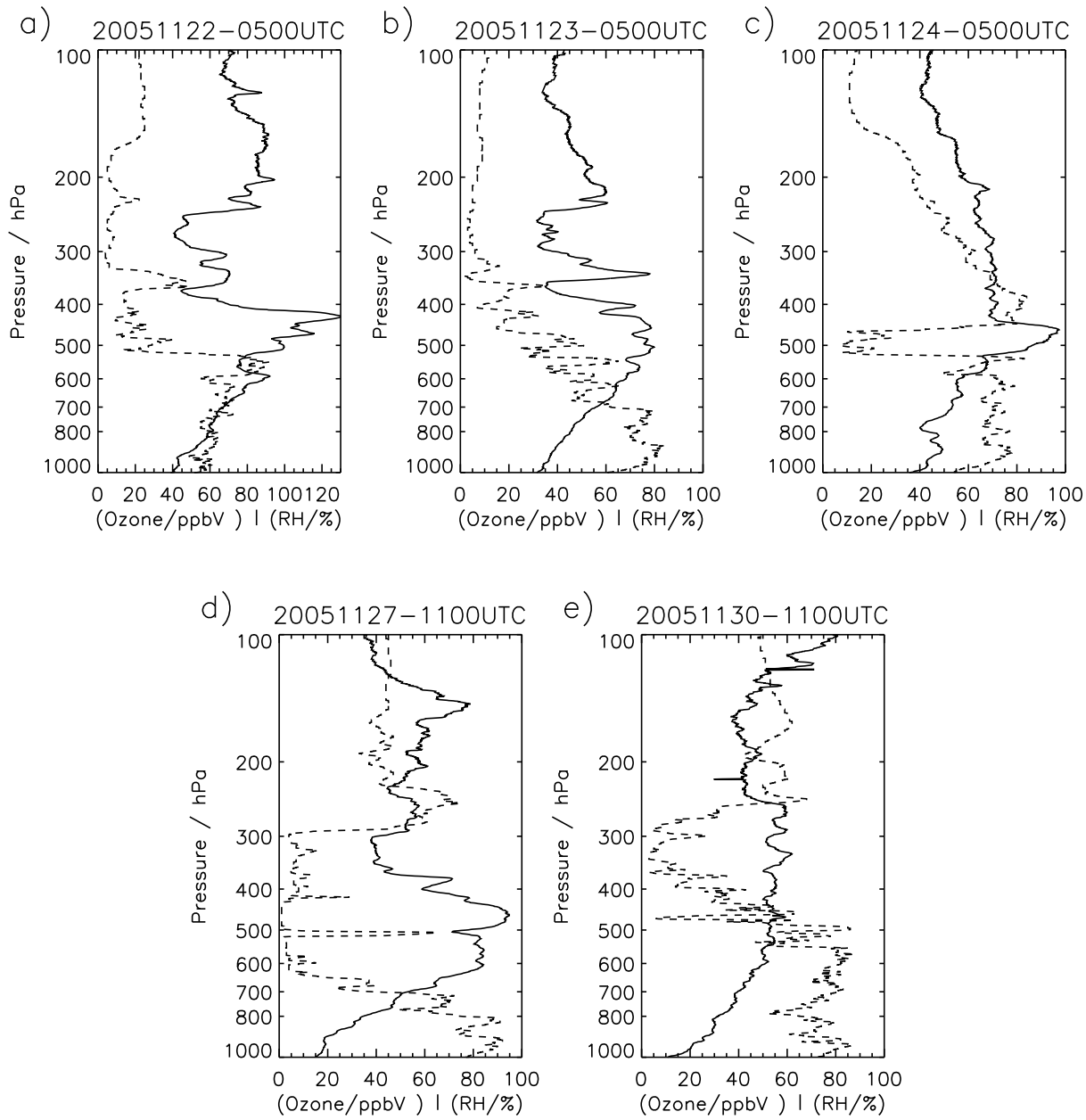

Figure 6. Vertical profiles of tropospheric ozone concentration and relative humidity (RH) over water ($> 0\,^{\circ}$C)) or over ice ($< 0\,^{\circ}$C) as appropriate, measured by ozonesondes launched from Darwin Airport between 22 and 30 November 2005 on the dates specified in each panel

that significant CIN needs to be present for deep convection to develop instead of widespread shallow convection.. Figure 10 shows a vertical-latitude cross-section of wet-bulb potential temperature (θ_w) and RH, calculated from ECMWF thermodynamic fields, through the $129\,^{\circ}$E meridian at 00 UTC (0930 local time) on 20 November 2005, again corresponding to the satellite image in Figure 8(c). This represents a cross-section through the TP, near the point of coastal initiation in Figure 8(a). The white dashed line marks the point where convection was seen to be initiated in Figure 8a. A warm and moist boundary layer is seen by the red contours in Figure 10 between $18\,^{\circ}$S and $6\,^{\circ}$S, but most importantly, a thin layer of much reduced θ_w ($\sim 290\ K$) and RH ($< 30\%$) between $920\ mb$ and $850\ mb$ is observed directly above the moist boundary layer at $14\,^{\circ}$S. Another such layer

Prepared using qjrms3.cls
DOI: 10.1002/qj

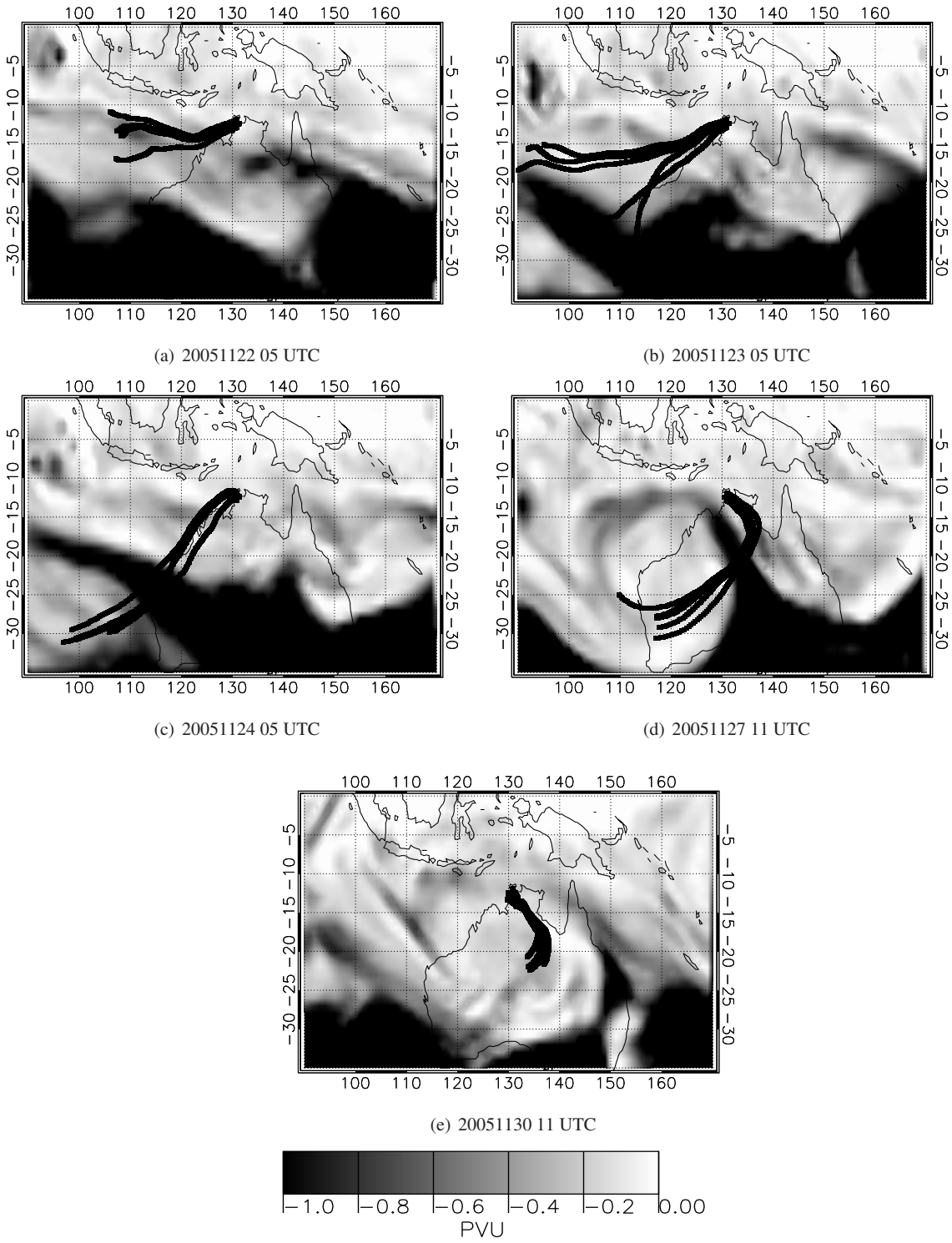

(a) 20051122 05 UTC

(b) 20051123 05 UTC

(c) 20051124 05 UTC

(d) 20051127 11 UTC

(e) 20051130 11 UTC

Figure 7. 0.5-degree clustered 4-day ECMWF back trajectories corresponding to layers of enhanced ozone observed in ozonesondes (Figure 6) launched from Darwin, ending at 500 hPa centred on 130.9,° E, 12.4,° S, over-plotted with ECMWF-derived PV fields at the isentropic surface at trajectory origin (indicated in each panel) for the dates indicated.

is observed at mid-levels between 600 mb and 500 mb. These strong decreasing gradients in θ_W with height represent regions of high potential instability. This potential instability was generated when the eastward-moving dry slot moved over the moist boundary layer two hours prior to the observed convection. A tephigram derived from ECMWF thermodynamic fields, corresponding to the location of the dashed white line in Figure 10, is

DOI: 10.1002/qj

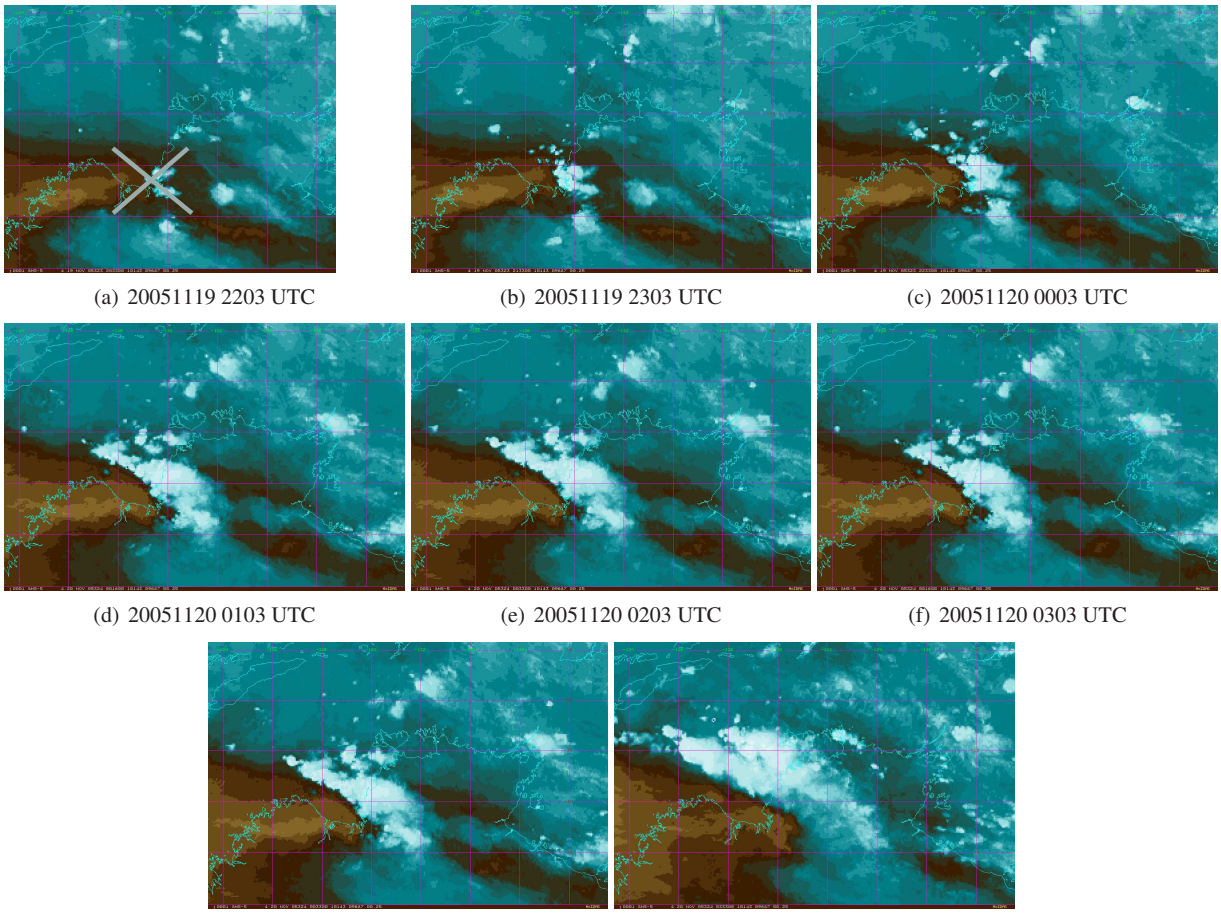

(a) 20051119 2203 UTC (b) 20051119 2303 UTC (c) 20051120 0003 UTC

(d) 20051120 0103 UTC (e) 20051120 0203 UTC (f) 20051120 0303 UTC

(g) 20051120 0403 UTC (h) 20051120 0503 UTC

Figure 8. A sequence of MTSAT-1R water vapour channel false-colour images over northern Australia at 1-hour intervals starting at 2203 UTC (0733 local +1 day), 19 Nov 2005 (upper left) showing the rapid development of a convective line near the boundary between moist (blue/white) and dry (brown/dark) airmasses. The cross in the first panel marks the point of convective initiation.

plotted in Figure 11. The two layers of reduced θ_w are evident in the tephigram as sharp reductions in the dew-point temperature profile (dot-dashed line) at 920 mb and again at 550 mb. The high CIN calculated for this profile (211 Jkg^{-1}) is clear from the strong temperature inversion (thick solid black line) at the top of the boundary layer (920 mb), which is coincident with the low-level dry layer. This region of high potential instability explains why convection occurred at 14 °S, but due to the high CIN, some forcing mechanism must have been required to realise the instability. On the coast, where convection was initiated in Figure 8(a), it is possible that land-sea breeze convergence may have generated the required forcing; however, this argument cannot apply to the observed isolated cells which developed over the ocean. Convectively-generated gravity waves trapped in the boundary layer (which do have phase speeds similar to those required) may have played a role in propagating the convective line as observed, for example, by Mapes (1993) in other organised tropical convective systems, possibly providing the necessary uplift required to release the same potential instability over the ocean. However, in the absence of any in-situ observations we cannot confirm or deny this speculation. Whatever the forcing mechanism, the evidence is clear - a synoptic scale tropical cloud system developed along a line of potential instability which was generated by an advecting dry slot. The origins of this dry slot are

DOI: 10.1002/qj

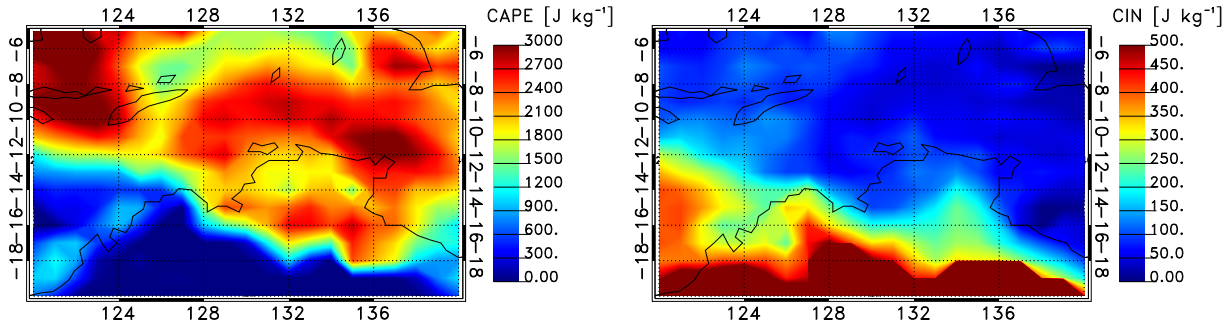

(a) (b)

Figure 9. Contours of: (a) Convective Available Potential Energy (CAPE); and (b) Convective Inhibition (CIN) over tropical northern Australia at 00 UTC on 20 November 2005, diagnosed from ECMWF analysis thermodynamic fields

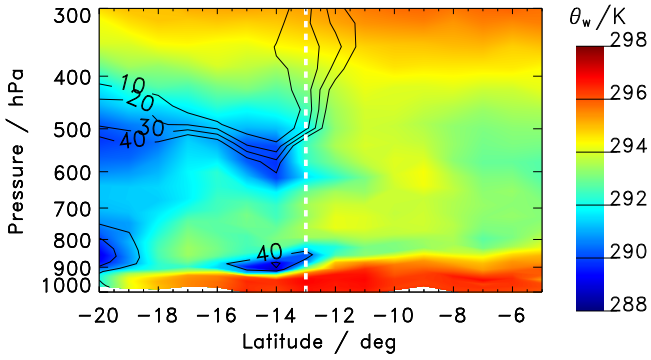

Figure 10. A cross-section in latitude of wet-bulb potential temperature (colour contours) derived from ECMWF analysis fields through the 129,° (E) meridian at 0930 local time on 22 November 2005. Labelled black contours define relative humidity isopleths. The dashed white line highlights 14,° (S)

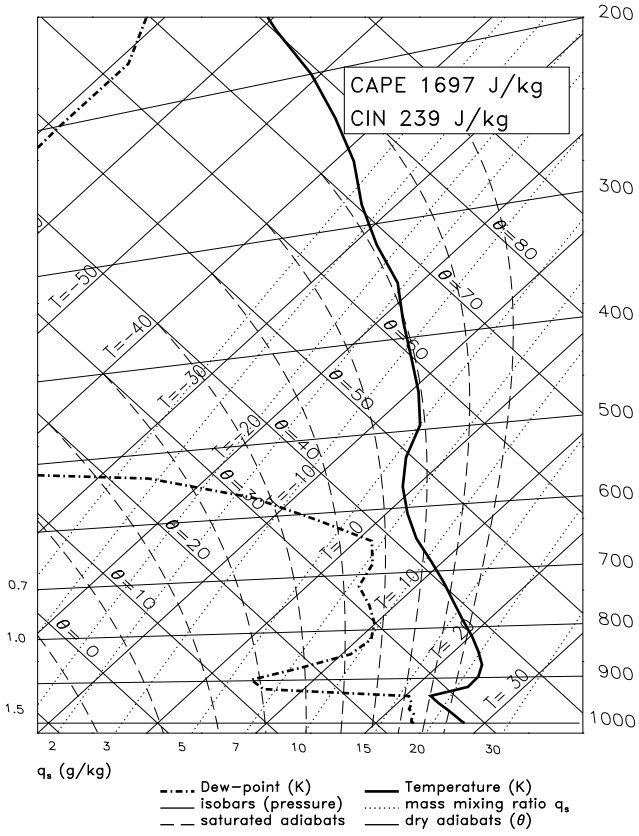

Figure 11. Tephigram at 00 UTC on 20 November 2005 at 129,° (E), 14,° (S) derived from ECMWF analyses. The solid black line defines ambient temperature, the dash-dot line showing dew point temperature. CAPE and CIN calculated for the surface parcels are indicated top right. The right-hand y-axis defines pressure (hPa).

now investigated further.

4.2.2 *Origins of the tropical dry slot*

Dry slots in the tropics are commonly observed meteorological features and have been linked to TPs in previous studies as discussed in Section 1. By their very nature, dry slots represent descending (or recently descended) airmasses. Analysis of ECMWF geopotential, temperature and wind fields at 150 mb (not shown here) showed that the tropical plume discussed here was not associated with a mobile upper level trough, a feature previously linked to TPs by Knippertz (2007) and McGuirk *et al.* (1988); however this plume does retain the commonly observed advancing dry slot. Four-day back trajectories initiated from within the unstable dry layer of reduced θ_w seen in Figure 10, are plotted in Figure 12. A PV field derived from ECMWF analyses is also plotted on the isentropic surface where the central trajectory terminated. These trajectories show that the unstable dry layer originated within

Prepared using qjrms3.cls
DOI: 10.1002/qj

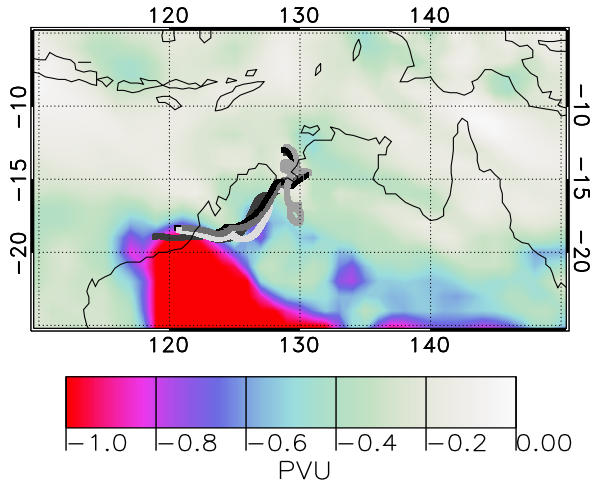

Figure 12. 0.5-degree clustered 4-day ECMWF back trajectories originating at 00 UTC on 20 November 2005, corresponding to the layer of potential instability at 900 mb (Figure 11) centred at 129,° (E), 14,° (S). ECMWF-derived PV fields (colour contours) are over-plotted on the 314 K isentropic surface at trajectory origin.

a tropopause fold (the finger of high PV at the end of the trajectories in Figure 12).

4.2.3 *Discussion of TP dynamics*

Knippertz (2007) notes that there are a number of different views currently in the literature (see his Section 5) concerning the relationship between convection/TPs and the existence of upper-level troughs, the key question being whether the observed lifting is a result of dynamical forcing, convective heating or some interaction between them. We suggest here that the tropical plume discussed in this study was not associated with an upper level trough and formed as a result of potential instability generated in the lower and mid-troposphere by the advection of very dry air over the moist tropical boundary layer. The low-level forcing mechanism required to overcome significant CIN and release this potential instability cannot be derived from the data available to this study, but may have been forced initially by sea-breeze convergence or by the nearby low-level trough discussed in Section 3.

5 Conclusions

Two tropical drought periods of reduced rainfall and cloud cover over tropical northern Australia were identified between 16 and 19 November and 23 and 27 November 2005 respectively. Both drought periods were found to be coincident with the descent of dry upper tropospheric air advected from the midlatitudes in tropopause folds associated with a series of breaking Rossby waves observed on the southern STJ. In the second drought period a double Rossby wave breaking event facilitated the penetration of upper tropospheric midlatitude air well into the tropics over northern Australia as far north as 10 °S; the first wave created a westerly wind duct for the latter to propagate further equatorward. Fields from ECMWF analyses and back trajectories confirm some at least of these layers originated in PV streamers of midlatitude origin generated by the Rossby waves. Satellite water-vapour imagery showed a resultant dry pool resided over a large area of North West Australia over both dry periods. In summary, despite the typically high tropical humidities of $70-80\%$ recorded by radiosondes in the Darwin boundary layer (up to around 700 mb), the dry, descending air measured at tropospheric mid-levels over Darwin inhibited convective activity for about 5 days over a wide area, except for coastal zones where strong sea-breeze convergence was able to remove this convective inhibition. In between the two dry periods and on the edge of another dry layer associated with a tropopause fold, a tropical cloud plume was observed to form rapidly along a boundary between moist and dry air seen in satellite water vapour images on 20 November 2005. This convection was initiated on the north west coast of Australia at 0730 local time on 20 November. The rapid development (6 hours) of this cloud structure was associated with the forced release of potential instability generated as dry air overrode moist

DOI: 10.1002/qj

air in the continental and maritime boundary layer. The initial forcing required to release this instability was probably a combination of land-sea-breeze interactions and a low-level trough which passed near the observed point of convective initiation on the coast. Subsequent independent convective development along this moisture gradient out to sea was too rapid to have propagated via gust fronts and its initiation remains an open question. We therefore conclude that breaking Rossby waves along the sub-tropical jet can affect tropical convection in two main ways: a) as the waves break they introduce into the tropical troposphere descending layers of very dry, ozone-rich air. In some cases these have high potential vorticity which manifests itself as high static stability which provides convective inhibition. In other cases the signature is purely one of composition, and the suppression of convection must then be due to entrainment of dry air into rising convective plumes. b) At the leading edges of the descending dry air potential instability can be released, leading to 'tropical plumes' of deep convection. The frequency of tropopause fold events and their potentially important impact on tropical convection, as demonstrated here, is currently poorly characterized. These observations support a growing number of studies linking midlatitude dynamics with the modulation of tropical deep convection and highlights the need for such processes to be considered in studies of tropical deep convective processes and tropical tropospheric chemistry and composition.

Acknowledgement

The ACTIVE campaign was funded by a Natural Environment Research Council consortium grant (NE/C512688). European Centre for Medium-Range Weather Forecasts (ECMWF) Operational Analysis data, were provided by the British Atmospheric Data Centre. Available from: http://badc.nerc.ac.uk/data/ecmwf-op/. Support for the MTSAST-1R analyses was provided by the Department of Energy ARM Program.

References

Blackwell KG. 2000. Tropical plumes in a barotropic model: a product of Rossby wave generation in the tropical upper troposphere. *Mon. Wea. Rev.* **128**, 2288-2302

Browning KA, and Roberts NM. 1994. Use of satellite imagery to diagnose events leading to frontal thunderstorms, Part 1. *Met. Apps.* **1**, 303-310

Browning KA, and Roberts NM. 1995. Use of satellite imagery to diagnose events leading to frontal thunderstorms, Part 2. *Met. Apps.* **2**, 3-9

Brunner D, Siegmund P, Peter T *et al.* 2008. Overview and meteorological context of the SCOUT-O3 aircraft measurement campaign in Darwin, Australia, Nov-Dec 2005, submitted to ???, April 2008

Danielsen EF. 1968. Stratospheric-tropospheric exchange based on radioactivity, ozone, and potential vorticity. *(*J. Atmos. Sci.) **25**, 502-518

Davidson NE, Tory KJ, Reeder MJ, *et al.* 2007. Extratropical-Tropical interaction during onset of the Australian Monsoon: Reanlysis diagnostics and idealized dry simulations. *J. Atmos. Sci.* in press.

Hoskins BJ, McIntyre EM, and Robertson AW. 1985. On the use and significance of isentropic potential vorticity maps. *Q. J. R. Meteorol. Soc.* **111**, 877-946

Hoskins BJ, and Ambrizzi T. 1993. Rossby wave propagation on a realistic longitudinally-varying flow. *J. Atmos. Sci.* **50**, 1661-1671

Kiladis GN. 1998. Observations of Rossby waves linked to convection over the eastern tropical Pacific. *J. Atmos. Sci.* **55**, 321-339

Knippertz P, 2005. Tropical-extratropical interactions associated with an Atlantic tropical plume and subtropical jet streak. *Mon. Wea. Rev.* **133**, 2759-2776

Knippertz P, and Martin JE. 2006. The role of dynamic and diabatic processes in the generation of cut-off lows over northwest Africa. *Meteorol. Atmos. Phys.* doi:10.1007/s00703-006-0217-4

Knippertz P. 2007. Tropical-extratropical interactions related to upper-level troughs at low latitudes, *Dyn. Atmos. Oceans.* **43**, 36-62

Mapes BE. 1993. Gregarious Tropical Convection. *J. Atmos. Sci.* **50**, 20262037. doi:10.1175/1520-0469

Mapes BE, and Zuidema P. 1996. Radiative-dynamical consequences of dry tongues in the tropical troposphere. *J. Atmos. Sci.* **53**, 620-638

McGuirk JP, Thompson AH, and Schaefer JR. 1988. An Eastern Pacific tropical plume. *Mon. Wea. Rev.* **116**, 2505-2521

DOI: 10.1002/qj

McGuirk JP, and Ulsh DJ. 1990. Evolution of tropical plumes in VAS water vapor imagery. *Mon. Wea. Rev.* **118**, 1758-1766

Morcrette C, Humphrey L, Browning KA, *et al.* 2007. Combination of Mesoscale and Synoptic Mechanisms for Triggering an Isolated Thunderstorm: Observational Case Study of CSIP IOP 1, *Mon. Wea. Rev.* **135**, 3728-3749

Minnis P. *et al.* 1995. Cloud Optical Property Retrieval (Subsystem 4.3). *Clouds and the Earth's Radiant Energy System (CERES) Algorithm Theoretical Basis Document, Volume III: Cloud Analyses and Radiance Inversions (Subsystem 4)*, NASA RP 1376 Vol. 3, edited by CERES Science Team, pp. 135-176

Minnis P, Nguyen L, Smith WL, *et al.* 2006. Large-scale cloud properties and radiative fluxes over Darwin during TWP-ICE. *Proc. 16th ARM Sci. Team Mtg., Albuquerque, NM, March 27-31.* ()

Parsons DB. 2000. Recovery Processes and Factors Limiting Cloud-Top Height following the Arrival of a Dry Intrusion Observed during TOGA COARE. *J. Atmos. Sci.*, textbf59, 2438

Parsons DB, Yoneyama K, and Redelsperger J-L. 2000. The evolution of the tropical western Pacific atmosphere-ocean system following the arrival of a dry intrusion. *Q. J. R. Meteorol. Soc.*, **126**, 517-548

Reid SJ, Vaughan G, Marsh ARW, and Smith SJ. 1996. Accuracy of Ozonesonde Measurements in the Troposphere. *J. Atmos. Chem.*, **25**, 215-226

Slingo JM, 1998. Extratropical forcing of tropical convection in a northern winter simulation with the UGAMP GCM. *Q. J. R. Meteorol. Soc.* **124**, 27-51

Vaughan G, Schiller C, MacKenzie AR, *et al.* 2008. Studies in a natural laboratory: High-altitude aircraft measurements around deep tropical convection. In press, *Bull. Amer. Meteorol. Soc.* 2008.

Yoneyama K, and Parsons DB. 1999. A proposes mechanism for the intrusion of dry air into the Tropical Western Pacific region. *J. Atmos. Sci.* **56**, 1524-1546

DOI: 10.1002/qj